Automatic Horizontal Curve Identification and Measurement Method Using GPS Data

Chengbo Ai[1] and Yichang (James) Tsai[2]

[1]School of Civil and Environmental Engineering, Georgia Institute of Technology, 790 Atlantic Dr. Atlanta, GA 30332. Email: chengbo.ai@gatech.edu

[2]School of Civil and Environmental Engineering, Georgia Institute of Technology, 790 Atlantic Dr. Atlanta, GA 30332.

ABSTRACT

Horizontal curves play a critical role in roadway safety by providing a smooth transition between tangent sections. Because radius of horizontal curves are one of the most fundamental elements in roadway geometry design, transportation agencies, e.g. state departments of transportation (DOTs), need to measure them to support network-level safety analysis. However, the traditional methods that are commonly used by transportation agencies, e.g. plan sheet reading method and chord-offset method, are time-consuming, labor-intensive, and inaccurate. Although some semi-automatic and automatic methods have been developed using global positioning system (GPS) data and/or geographic information system (GIS) functions in recent years, these methods are not yet ready to be practically used in a network-level analysis because they either require intensive manual intervention, or lack of the capability in automatically identifying complex curves. This study is aimed to develop a new method using widely available GPS data that can automatically identify all types of horizontal curves and measure the corresponding curve radii, including the most challenging spiral curve. The simulation test using 385 synthetic horizontal curves shows that the proposed method can correctly identify 90.1% of the tested curves and can accurately classify 87.3% of the detected curves types. The field test shows that the proposed method can correctly

identify all of the 25 tested curves, and can accurately measure the corresponding radii. The results from an experimental test clearly demonstrate the accuracy and effectiveness of the proposed method. A case study on Interstate 285 demonstrates that proposed method is a promising method for transportation agencies to achieve reliable and efficient network-level analysis.

INTRODUCTION

Horizontal curves are one of the most important elements in roadway geometry design. The main function of a horizontal curve is to provide a smooth transition between two tangent roadway sections to ensure roadway driving consistency. Unfortunately, a disproportional number of serious vehicle crashes occur at horizontal curves despite the fact that curves only represent a fraction of the roadway network. As reported by the Federal Highway Administration (FHWA) Office of Safety, 27% of fatal crashes occurred at horizontal curves in the years of 2006-2008 (FHWA 2010). Nationwide research has been conducted to better understand how the characteristics of horizontal curves could be related to crashes and how countermeasures can be effectively applied to reduce crash rates (Lin 1990). A major lesson learned from the research is that transportation agencies need an accurate inventory of horizontal curve locations and the corresponding geometry measurements to implement their road safety analysis and improvement program.

However, even though analytical models (e.g. SafetyAnalyst, by the American Association of State Highway and Transportation Officials (AASHTO)) and data specifications (e.g. the Model Inventory of Roadway Elements (MIRE) by FHWA) have been developed to facilitate roadway safety analysis, very few public transportation agencies are able to use the database in an effective and efficient manner because it does not have complete and accurate horizontal curve location and geometry information. Traditionally, public transportation agencies use a plan reading method and/or a chord offset method to determine a specific roadway curve radius. Due to the nature of these methods, the process can be time-consuming and labor-intensive for field engineers.

In recent research, several methods have been developed using ArcGIS roadway Shapefile in the ArcMap environment (Drakopoulos and Örnek 2000; Hans et al. 2012). Although these methods include several convenient user interfaces for engineers to operate, they still require

manual digitization of the point of curve (PC) and the point of tangent (PT) for each curve to obtain a reliable measurement, which results in a large workload and low productivity. It is impractical and non-economical for transportation agencies to directly adopt these existing methods for their network-level analysis. To take advantage of the programmable capability in ArcGIS and to improve the efficiency, there have been two attempts to develop automatic curve identification and measurement: the "Curve Finder" developed by New Hampshire DOT (NHDOT) (Findley et al. 2012) and the "CurveFinder" developed by Li et al. (2012). While both of these methods demonstrated reasonable results in an automatic manner for simple curves, both have challenges in processing complex curves, which hinders many transportation agencies from immediately using them.

The objective of this paper is to develop an automatic horizontal curve identification and radius measurement method that is effective for all four common types of horizontal curves (simple curves, compound curves, reverse curves, and spiral curves) by using the global positioning system (GPS) trajectory data that are widely available in many transportation agencies.

LITERATURE REVIEW

Recognizing the traditional methods used by transportation agencies can be time-consuming, labor-intensive, and inaccurate, some researchers have attempted to develop methods that can automatically conduct horizontal curve identification and measurement by introducing different data sources and computational methods. A ball bank indicator and digital compass (Carlson et al. 2005; Milstead et al. 2011) have been employed to record the lateral acceleration and vehicle heading changing rate along a curve so that the curve radius can be back-calculated based on the point-mass equation and radian measures. Although the radius of the curve is simple to calculate and the results are reasonable, these methods can only be applied to small-scale projects, such as curve advisory speed determination, because they require not only the PC and PT stations established on site before the test, but also the testing vehicles must be driven at a constant speed throughout the curve (Pratt et al. 2009). With the advances in geographic information system (GIS) and the wide availability of the GPS data, the spatial analysis method becomes a feasible,

cost-effective option for roadway curve identification and measurement. Researchers have started to employ a GIS approach to calculate the radii of curves from the digital road network (Rasdorf et al. 2012). The interactive interfaces created on the ArcGIS platform, e.g. the Curve Calculator by Environmental Systems Research Institute (ESRI 2010) and the Curvature Extension by the Florida Department of Transportation (FDOT 2010), conveniently enable users to select the PC and PT points of the curve; the corresponding radius will then be computed by automatically extracting the arc and chord length of the curve from a GIS map. Image-based approaches have also been developed using either rectified ortho-imagery (Dong et al. 2007; Easa et al. 2007) or calibrated video log images (Tsai et al. 2010). However, extensive labor is still required for these methods, which hinders their application in network-level analysis.

As pointed out in previous section, only two methods have been found in previous literature that have attempted to automatically identify and measure horizontal curves with minimum manual intervention. They are the "Curve Finder" developed by NHDOT and the "CurveFinder" developed by Findley et al. (2012). The "Curve Finder" by NHDOT (Findley et al. 2012) defines an error quotient that expresses how well a curve is defined. Three consecutive GPS points are used to estimate a small circle, while a series of these circles forms a circle cluster that can potentially define a curve. The error quotient is calculated by the average of the distance from the center of each circle to the center of the cluster and then normalized by the overall radius. Hence, a zero error means a perfect fit of every circle within the cluster, while a large error indicates that the circles within the cluster are unlikely to form a curve. This method primarily works well on simple curves, but it is very challenging for this method to identify and measure complex curves because the circle estimation uses only three points and is no longer robust enough to capture the transition among different curved segments within the complex curve. The "CurveFinder" by Findley et al. (2012) defines a threshold for the bearing angle to differentiate the curved sections from the tangent sections. The bearing angle is computed consecutively using three adjacent points along the roadmap and compared with the calibrated threshold. A corresponding add-in using ArcGIS programming package ArcObjects was developed to facilitate the operation of road layer selection,

results query, and selection, etc. Using the selected testing dataset, the "CurveFinder" can correctly identify 96.7% of the tested curves. However, the "CurveFinder" can only differentiate two curve types, the simple curve and compound curve, and it only demonstrates a 79% classification rate due to the limited precision of the bearing angles computed by the three consecutive points.

In summary, the existing methods in previous studies have demonstrated their potential and effectiveness in extracting horizontal curves. However, the existing methods either still require extensive manual inputs or still need improvement in identifying and classifying complex curves. Consequently, this paper is aimed at developing automated horizontal curve identification and measurement method that can minimize manual input and that is effective for identifying all types of curves.

METHODOLOGY

The segment is considered as the minimal unit in this paper that has a single radius. A curved segment has a radius of R (a curvature of R^{-1} while a tangent segment has a radius of infinity (a curvature of zero). A simple horizontal curve consists of curved segments and tangent segments delineated by PC and PT, as shown in Fig. 1(a). For more complex horizontal curves, there are adjacent curved segments or separated curved segments divided by inner tangent segments, e.g. a reverse curve shown in Fig. 1(b). The objective of this study is to accurately identify the curved and tangent segments, to reliably cluster the corresponding segments into different horizontal curve types and to measure the corresponding radii along the identified curve.

The proposed horizontal curve identification and measurement method in this paper consists of three key steps. First, the GPS trajectory data that represents the roadway is sequentially processed and segmented into delineated segments using iterative circular fitting. Second, the delineated segments are further clustered into curve sections and classified into different curve types based on their spatial distribution and adjacency. Third, the radii that correspond to each curve are computed. Especially, the radii along spiral curves are updated using a spiral fitting instead of the aforementioned circular fitting. Fig. 2 shows the flowchart of the proposed method. Before discussing these three key steps, the characteristics of the GPS trajectory data used in this study

and the step of post-processing are briefly discussed, as shown in dashed boxes in Fig. 2.

Characteristics of GPS Trajectory Data and Post-Processing

The GPS trajectory data used in this study is collected using a sensing vehicle developed by Georgia Tech. Fig. 3 shows a picture of the sensing vehicle and an example of the collected GPS trajectory data. In this study, the raw GPS trajectory data is acquired at the frequency of 5Hz at around a 60mph driving speed. Because the data is collected through a mobile platform, many factors will impact the accuracy of the raw GPS trajectory data, e.g. the dilution of precision (DOP), temporary satellite loss, limited dwell time, etc. Therefore, the raw GPS trajectory data needs to be post-processed through differential adjustment and triangulation using base station data collected by the continuous operating reference stations (CORS) to reduce the impact of these negative factors on the accuracy. While inertial navigation system (INS) data is not essential in the proposed method, it can be used to compensate for the loss of GPS data at the locations where satellites are not visible, e.g. in a tunnel. There are many commercially available software products for conducting GPS data post-processing, e.g. Topcon Tools, Leica GeoOffice, etc. In this particular study, Applanix POSPac MMS software is used to post-process the GPS data. The post-processed GPS trajectory data is the input of the proposed algorithm in this study.

Roadway Segmentation

The objective of roadway segmentation is to automatically partition the GPS trajectory data that represents the roadway into delineated segments. Each segment shares the same radius measurement. The iterative process is proposed to ensure that an optimized number of GPS points are grouped for each segment, while the circular fitting process is introduced to improve the robustness of the measurement to the disturbances in GPS points. In previous studies, automatic circular fitting methods have been proposed with accurate results (Kasa 1976; Pratt 1987; Taubin 1991). However, it is not feasible to directly apply these methods for horizontal curve radius measurement without identifying the delineation of the roadway. These circular fitting methods only take a fixed number of points for circular fitting. Hence, no matter how robust the circular fitting method is, the fitting results are severely biased by the selected number of points.

In this paper, an iterative circular fitting algorithm is proposed to the GPS points to obtain the initial circular fitting results. Fig. 4 shows the pseudo code for the iterative circular fitting and an example of how the iterative fitting converges to an optimal group of GPS points for each segment. Instead of selecting a fixed number of neighboring points for fitting, incremental number of neighboring points are attempted until arriving at the least fitting error. The number resulting in the least fitting error will be associated with this group of GPS points (i.e. L_n). The fitting error is measured by the fitness of the actual GPS points compared to the approximated circle. As shown in Fig. 4, the error curve is monitored and recorded separately until the global minimal value is arrived at among all the attempted iterations. Once the number of neighboring points is selected for the current group of GPS points (i.e. L_n), the next circular fitting will be started by skipping the current group of points. Hence, optimized numbers of GPS points are selected for each group of GPS points (i.e. segment) through iterations.

In this paper, the classic circular fitting method proposed by Kasa (1976) is selected for its computational efficiency and robustness to noise. The circular fitting method proposed by Kasa defines a minimization problem of the least square error between the sample points used for circular fitting and the approximated circle. The detailed description and the key equations in this method are derived in Appendix I. Fig. 5 shows an illustration of the resultant segments derived from the iterative circular fitting. The alternative colors used in the figure are to highlight the delineation. A single radius measurement is associated with all the GPS points within the same segment. Whether or not the delineated segment is curved or tangent will be determined in the subsequent steps.

Curve Identification

The objective of curve identification is to automatically identify the horizontal curve and the corresponding curve types using the delineated segments derived from the previous step and based on the spatial distribution and adjacency of these segments.

Segment Type Identification: The types of the delineated segments are first determined using the center angle Δ. Fig. 6 shows the illustration of different center angles for curved and tangent segments. The center angle of the delineated segment can be computed using the fundamental arc

length equation for circles, and the arc length can be estimated from the GPS acquisition parameter or directly obtained from the distance measurement instrument, as shown in the following equation (Eq. 1):

$$\Delta_n = \frac{S_n}{R_n} = \frac{\sum_{i=1}^{m} \frac{v_i}{f}}{R_n} \tag{1}$$

where:

Δ_n - The center angle of the nth segment in radian;

R_n - The radius computed by the iterative circular fitting for the nth segment;

S_n - The arc length for the nth segments;

m - The number of GPS points (i.e., interval) included in the nth segments;

v_i - The instantaneous vehicle speed acquired by GPS at the ith point;

f - The GPS acquisition frequency.

- For tangent segments, the error from the circular fitting will not be reduced by increasing the number of neighboring GPS points for circular fitting. Therefore, the group representing a tangent segment typically contains very few GPS points m and bears a large radius Rn, hence an extremely small center angle Δ_n;
- For curved segments, the error from the fitting will be reduced by increasing the number of GPS points until the selection of GPS points starts to include tangent sections. Therefore, the group representing a curved segment typically contains more GPS points m and results in a relatively small radius Rn, hence a relatively large center angle Δ_n.

An appropriate chosen Δ_n will impact the performance of the identifications of tangent segments and curved segments, hence the performance of the curve identification. Therefore, a parameter calibration process is needed to determine the optimal threshold of Δ_n. In this study, six roads were selected from the Savannah area in Georgia as the source of the calibration data and covering different functional classes, e.g. interstate highway, state route and local road. The corresponding GPS trajectory data was collected and used to digitize the curves on these roads. The proposed iterative circular fitting was applied to segment the GPS trajectory data into delineated segments.

A manual review was then conducted to determine whether the delineated segment is a tangent segment or a curved segment by correlating the segments to the manual digitization results. In total, 47 curve segments and 194 tangent segments were manually determined. Fig. 7 shows the distribution of the center angle Δ_n for these manual results. As shown in Fig. 7, the center angles derived from the tangent segments never exceed 5° , while the minimum center angle derived from the curved segments is 7.8° . Therefore, the threshold for the center angel Δ_n can be determined based on the distribution. In this paper, the GPS acquisition frequency f is configured at 5Hz and the threshold is set at 5° . Following the same procedure for practical use, transportation agencies can calibrate their parameter if the data acquisition frequency is different from this paper.

Curve Classification: The validated curved and tangent segments are then classified into different curve types according to their adjacency patterns. Fig. 8 shows the typical patterns for different curve types. Regardless of the curve type, there is always a back and forward tangent segment that enters and exits the center curved segment(s), respectively (i.e. shown in black color in Fig. 8). Therefore, the pattern of the center curved segment(s) (i.e. shown in light and dark gray colors in Fig. 8) determines the curve types:

- Non-curve (Straight): consecutive tangent segments are presented;
- Simple curve: a single curved segment is presented;
- Compound curve: two curved segments with the same curve direction are presented;
- Reverse curve: two curved segments with opposite curve directions are presented;
- Spiral curve: three curved segments with the same curve direction and symmetric curvature measurements are presented.

Spiral Curve Update

In previous steps, spiral curves are first identified as three consecutive curves, where the back and forward spirals are simplified using two simple curves with smaller curvatures. However, because the curvature of the spiral curve changes linearly with its curve length, circular fitting results in previous steps for these two spirals need to be updated. The Clothoid spline method by Meek and Walton (1992) is used to approximate the spirals. From previous steps, the back spiral

is connected between the ending point of the back tangent segment (TS) and the starting point of the center curve (SC), while the forward spiral is connected between the ending point of the center curve (CS) and the starting point of the forward tangent segment (ST). The detailed description and the key equations in the Clothoid spline method are presented in Appendix II.

As the equation for each identified curve has already been modeled in the step of iterative circular fitting and validated in the step of curve identification, the corresponding measurement of curvature (i.e. radius) is already computed and associated with each point of the GPS trajectory. By updating the curvature measurement at each point at spiral curves in this step, the horizontal curve identification and measurement processes are complete.

EXPERIMENTAL TEST

The objective of the experimental test is to comprehensively evaluate the performance of the proposed method for curve identification and measurement. Simulation tests using synthetic curve data were performed first to evaluate the accuracy of the proposed method in terms of type identification. Field tests using real-world curve data are then conducted to evaluate the performance of the proposed method in terms of measurement by comparing them with ground truths derived from satellite imagery.

Simulation Test for Curve Identification

The objective of the simulation test is to assess the accuracy of the curve identification. Because it is challenging to prepare a comprehensive dataset from the real world with all types of curves, especially the complex curves, a comprehensive synthetic dataset was created sequentially by inserting synthetic road sections with a known geometry formula. The synthetic data is then sampled into discrete synthetic GPS trajectory. To be consistent with the reality, the synthetic dataset is dimensioned to the scale of the real world curves, and the GPS trajectory is then discretized based on the GPS acquisition frequency of 5Hz and the default driving speed of 60mph. In order to test the robustness of the proposed method, several types of GPS disturbances observed from the real GPS tracks are simulated in the synthetic data, including random GPS errors, missing GPS points, and local vehicle maneuvering. These GPS disturbances can locally interrupt the continuity of the

GPS trajectory. In total, there are 385 curves generated for this simulation test. The accuracy in the simulation test is evaluated by both the detection performance and the classification performance.

For the detection performance, Type 1 (false negative, a failure to detect an existing curve) and Type 2 (false positive, a misidentification of a straight section as a curve) errors are used. A Type 1 error is reported when a curve in the ground truth is completely missed, or the detected curve section overlaps less than seventy-five percent of the corresponding ground truth, while a Type 2 error is reported when a detected curve section is complete at the straight section in the ground truth. It is noted that only 38 Type 1 cases and 27 Type 2 cases were identified, resulting in a correct detection rate of 90.1%. It should also be noted that out of the 38 Type 1 errors, there are only 10 curves that were completely missed, while the remaining 28 curves were still partially detected by the proposed method.

For the classification performance, a confusion matrix is used to evaluate how the proposed method distinguishes different curve types. The confusion matrix is derived based on the results from the detection results. A total of 347 curves that were correctly detected were tested for classification. Table 1 shows the confusion matrix results among different types. It can be observed from the diagonal cells of the confusion matrix that the proposed method demonstrates an overall good performance in differentiating the four curve types. Overall, 87.3% of the detected curves are correctly classified by the proposed method. Even for the challenging spiral curves, the proposed method achieves a 63.3% correct classification rate. However, 36.7% of the spiral curves were incorrectly classified as simple or compound curves due to the incorrect delineation between the center curve and its corresponding spirals. If both the forward and back spirals are incorrectly delineated, a misclassified simple curve will be reported, while if either of the spirals is incorrectly delineated, a misclassified compound curve will be reported.

Field Test for Curve Measurement

The objective of field test is to evaluate the performance of the proposed method in curve measurement. Three testing datasets were collected, including 25 simple curves with different radii. The corresponding GPS data was collected on these three roads. Fig. 9 shows the map of the

selected roadways.

- Georgia Tech Savannah campus: Georgia Tech Savannah campus contains consistent curve radius on a circular loop road (i.e., 5 radii ranging between 968 ft. to 1024 ft.);
- Jimmy Deloach Parkway: Jimmy Deloach Parkway is a minor arterial with many large and smooth curves (i.e. 10 radii ranging between 1409 ft. to 5596 ft.);
- Industrial Park Road: Industrial Park Road is a local road with many sharp curves (i.e. 10 radii ranging between 218ft. to 801ft.).

The satellite imagery for the selected testing datasets was used to digitize the ground truth using ERDAS and measure the accurate curve radius using AutoCAD. The proposed method was then applied to the three testing datasets. All of the 25 simple curves were correctly detected and the corresponding radius was automatically measured by the proposed method. Fig. 10 shows the scatter plot of the radius measurements derived from the proposed method against the ground truth measurements derived from AutoCAD. A linear regression with zero intercept was performed to demonstrate the correlation of the two results, shown as the solid line in Fig. 10. The slope of 1.0127 and the R^2 of 0.9999 strongly suggest an accurate measurement using the proposed method.

CASE STUDY: AN INTERSTATE 285 APPLICATION

Horizontal curve is one of the most important and fundamental elements in roadway geometry design. Not only the measured radius is critical information by itself for assessing the adequacy of the roadway design in a network level, but, more importantly, integrating the measured radius with other roadway geometry elements will provide a more meaningful safety-related product for transportation agencies. This case study is presented to demonstrate the usefulness of the proposed method in analyzing the adequacy of the roadway to avoid lane departure accidents. According to the policy on geometry design of highway and streets by AASHTO (2011) (Eq. 2):

$$f_s = \frac{v^2}{15 \cdot R} - e \tag{2}$$

where:

f_s - The side friction demand;

e - The rate of roadway super-elevation, ft./ft.;

v - The vehicle speed, mph;

R - The curve radius, ft.

The complete I-285 in Atlanta, Georgia, covering 63 miles, was collected for this case study. Fig. 11(a) shows curve radius (R) along I-285 derived from the proposed method. By applying the super elevation measurement (e) derived from Tsai et al. (2013) and the driving speed (v) obtained from the Georgia Department of Transportation (GDOT), the side friction demand along I-285 can be computed automatically. By comparing the computed side friction demand with a maximum side friction demand defined by stakeholders, the locations with potential safety concerns can be immediately identified. The maximum side friction demand can be flexibly adjusted by stakeholders, or replaced by the actual friction supply at the pavement-tire interface if the data is available. Fig. 11(b) shows an example map of the locations of interest where the maximum side friction demand of 0.12 is defined. These identified locations are informative for transportation agencies to further conduct on-site measurement and inspection. It should be noted that using the proposed method the complete process of the I-285 data (i.e. 63 miles) from the raw GPS data collection to the final result delivery only takes approximately six hours. In comparison, despite the necessity of establishing traffic control at some locations and the travel time between different curves, the chord-offset method and the GPS-based method by Carlson et al. (2005) will take at least half an hour to measure a single curve. The proposed method clearly shows the advantages as a more efficient and practical alternative for network-level analysis.

CONCLUSIONS AND RECOMMENDATIONS

In this paper, an automatic horizontal curve identification and measurement method using GPS data is proposed. The proposed method can accurately and efficiently identify different horizontal curve types, including the spiral curve, and accurately measure the corresponding radius. The conclusion this paper is summarized as follows:

- In the simulation test, the proposed method successfully detected 347 curves of different types out of a total of 385 curves in the dataset (i.e. 90.1% detection rate), while only 27 Type 2 errors were identified. An overall 87.3% of the detected curves were correctly classified into their corresponding types, including 63.3% of spiral curves that are challenging for the existing methods of detection in previous literature.
- In the field test, the proposed method not only successfully detected all of the selected 25 simple curves, but also accurately measured the corresponding radii compared with the digitization results using AutoCAD.
- The case study on I-285 has demonstrated that the proposed method has the capability to conduct a network-level analysis efficiently. The results derived from the proposed method show that the method can adequately support state DOTs' network-level safety analyses.

The following are the recommendation for future research:

- Future study is recommended to further reduce the Type 1 and 2 errors in curve detection and to further improve the spiral curve classification performance by improving the delineation of the back and forward spirals.
- Future study is recommended to adapt the proposed method to other road types whose curves might not be constructed under highway geometry design standard, e.g. log route, fire path, etc.
- Future on-site data collection of the side friction measurement is recommended to further validate the identified locations in the case study on I-285. The crash data, evidences of crashes or severe maneuvering (i.e. tire steering mark, etc.) are also recommended to be explored and inspected to further validate the identified locations. Additional safety-related applications should be explored by taking advantage of the derived continuous curve radius measurements from the proposed method.

APPENDIX I. KASA'S METHOD

Given a point set $(x_i, y_i), i \in (1, 2, \ldots, N)$ for circular fitting, where d_i is the distance between each point and the center of the fitted circle (A, B) in Eq. 3:

$$d_i^2 = (x_i - A)^2 + (y_i - B)^2 \tag{3}$$

The error between the edge of the fitted circle and the corresponding (x_i, y_i) is δ_i in Eq. 4:

$$\delta_i = d_i^2 - R^2 = (x_i - A)^2 + (y_i - B)^2 - R^2 = x_i^2 + y_i^2 + ax_i + by_i + c \tag{4}$$

Let

$$Q(a, b, c) = \sum \delta^2 = \sum \left(x_i^2 + y_i^2 + ax_i + by_i + c\right)^2 \tag{5}$$

The objective is to derive a, b and c so that $Q(a, b, c)$ is minimized. As $Q(a, b, c)$ is none negative, it has a minimal value only when Eq. 6 holds:

$$\begin{aligned} \frac{\partial Q(a,b,c)}{\partial a} &= \sum 2\left(x_i^2 + y_i^2 + ax_i + by_i + c\right) x_i = 0 \\ \frac{\partial Q(a,b,c)}{\partial b} &= \sum 2\left(x_i^2 + y_i^2 + ax_i + by_i + c\right) y_i = 0 \\ \frac{\partial Q(a,b,c)}{\partial c} &= \sum 2\left(x_i^2 + y_i^2 + ax_i + by_i + c\right) = 0 \end{aligned} \tag{6}$$

By solving Eq. 7:

$$\begin{aligned} a &= \frac{HD-EG}{CD-D^2} \\ a &= \frac{HC-ED}{D^2-GC} \\ c &= \frac{\sum\left(x_i^2+y_i^2+a\sum x_i+b\sum y_i\right)}{N} \end{aligned} \tag{7}$$

where (Eq. 8)

$$\begin{aligned} C &= N\sum x_i^2 - \left(\sum x_i\right)^2 \\ D &= N\sum x_i y_i - \left(\sum x_i\right)\left(\sum y_i\right) \\ E &= N\sum x_i^3 + N\sum x_i y_i^2 - \sum\left(x_i^2 + y_i^2\right)\left(\sum x_i\right) \\ G &= N\sum y_i^2 - \left(\sum y_i\right)^2 \\ E &= N\sum y_i^3 + N\sum x_i^2 y_i - \sum\left(x_i^2 + y_i^2\right)\left(\sum y_i\right) \end{aligned} \tag{8}$$

Therefore, the center (A, B) and the radii R of the fitted circle can be computed by Eq. 9.

$$\begin{aligned} A &= -\tfrac{a}{2} \\ B &= -\tfrac{b}{2} \\ R &= \tfrac{1}{2}\sqrt{a^2 + b^2 - 4c} \end{aligned} \tag{9}$$

APPENDIX II. CLOTHOID SPLINE METHOD

Fig. 12 shows the setup of the Clothoid spline with a back spiral. The objective is to determine the back spiral function between TS and SC, given the expected starting location of the spiral P and the starting (SC) and ending of the center curve (CS). The computation for the forward spiral follows the same steps without losing any generality.

Where:

K_P - The Unit curvature entering the spiral, $K_P = 0$;

K_Q - The Unit curvature exiting the spiral, K_Q = curvature of the center curve;

B - The scaling factor of the curvature.

The spiral can be represented using Fresnel integral (Meek and Walton 1992) in Eq. 10:

$$\pi B \begin{pmatrix} C(t) \\ S(t) \end{pmatrix} \tag{10}$$

where πB is the scaling factor and $C(t)$ follows Eq. 11:

$$C(t) = \int_0^t \cos\left(\frac{\pi}{2}u^2\right) du \tag{11}$$

The center of the center curve can be computed based on the circular arc function, and can also be computed based on the spiral in Eq. 12.

$$\begin{aligned} x + \tfrac{\pi}{K_Q} C^1 \sqrt{W - L} &= Q_1 - \tfrac{1}{K_Q}\sin(\tfrac{\pi}{2}W) \\ \tfrac{\pi}{K_Q} S^1 \sqrt{W - L} + \tfrac{1}{KQ} &= Q_2 - \tfrac{1}{K_Q}\cos(\tfrac{\pi}{2}W) \end{aligned} \tag{12}$$

where:

$\frac{\pi}{2}L$ - The angle of the center curve

$\frac{\pi}{2}W$ - The angle of the starting of the back spiral with respect to the horizontal

x - The distance between TS and P.

Since the locations of P and SC are given and the L is computed by the previous circular fitting, the spiral curve can be computed by solving the above equations for W and x. With the computed W and x, the total length of the spiral (S_0) can be computed. To effectively represent and record the approximated spiral curve, slope factor k, together with the location of TS and SC, are recorded for each spiral curve in this paper (Eq. 13).

$$k = \frac{S}{\frac{1}{R}} = \frac{S_0}{\frac{1}{R_0}} = S_0 \cdot K_Q \cdot B \tag{13}$$

where:

S - The length from a certain point to its initial position along the spiral

R - The radius at a certain point of the spiral curve

R_0 - The radius of the center curve (i.e. end of the spiral curve), equals $t = K_Q B$.

REFERENCES

AASHTO (2011). *A policy on geometric design of highways and streets-2011*. American Association of State Highway and Transportation Officials, Washington D.C.

Carlson, P., Burris, M., Black, K., and Rose, E. (2005). "Comparison of radius-estimating techniques for horizontal curves." *Transportation Research Record: Journal of the Transportation Research Board*, 1918, 76–83.

Dong, H., Easa, S., and Li, J. (2007). "Approximate extraction of spiralled horizontal curves from satellite imagery." *Journal of Surveying Engineering*, 133(1), 36–40.

Drakopoulos, A. and Örnek, E. (2000). "Use of vehicle-collected data to calculate existing roadway geometry." *Journal of Transportation Engineering*, 126(2), 154–160.

Easa, S., Dong, H., and Li, J. (2007). "Use of satellite imagery for establishing road horizontal alignments." *Journal of Surveying Engineering*, 133(1), 29–35.

ESRI (2010). *GIS for highways*, <http://www.esri.com/industries/highways> (April 14, 2014).

FDOT (2010). *Geographic information system application manager - curvature extension*, <http://www.dot.state.fl.us/planning/statistics/gis/> (April 14, 2014).

FHWA (2010). *Roads and curves, 2005-2008* (July, 2010).

Findley, D. J., Hummer, J. E., Rasdorf, W., Zegeer, C. V., and Fowler, T. J. (2012). "Modeling the impact of spatial relationships on horizontal curve safety." *Accident Analysis & Prevention*, 45, 296–304.

Hans, Z., Souleyrette, R., and Bogenreif, C. (2012). "Intrans project 10-369: Horizontal curve identification and evaluation." *Report no.*, Iowa DOT.

Kasa, I. (1976). "A circle fitting procedure and its error analysis." *IEEE Transactions on Instrumentation and Measurement*, IM-25(1), 8–14.

Li, Z., Chitturi, M., Bill, A., and Noyce, D. (2012). "Automated identification and extraction of horizontal curve information from geographic information system roadway maps." *Transportation Research Record: Journal of the Transportation Research Board*, 2291, 80–92.

Lin, F. (1990). "Flattening of horizontal curves on rural two-lane highways." *Journal of Transportation Engineering*, 116(2), 181–186.

Meek, D. S. and Walton, D. J. (1992). "Clothoid spline transition spirals." *Mathematics of Computation*, 59, 117–133.

Milstead, R., Qin, X., Katz, B., Bonneson, J., Pratt, M., Miles, J., and Carlson, P. (2011). "Fhwa-sa-11-22: Procedures for setting advisory speeds on curves." *Report no.*, Federal Highway Administration.

Pratt, M. P., Miles, J. D., and Bonneson, J. A. (2009). "Fhwa/tx-10/5-5439-01-1: Workshop on using the gps method to determine curve advisory speed." *Report no.*, Texas Transportation Institute.

Pratt, V. (1987). "Direct least-squares fitting of algebraic surfaces." *SIGGRAPH Comput. Graph.*,

21(4), 145–152.

Rasdorf, W. J., Findley, D. J., Zegeer, C. V., Sundstrom, C. A., and Hummer, J. E. (2012). "Evaluation of gis applications for horizontal curve data collection." *Journal of Computing in Civil Engineering*, 26(2), 191–203.

Taubin, G. (1991). "Estimation of planar curves, surfaces, and nonplanar space curves defined by implicit equations with applications to edge and range image segmentation." *IEEE Transactions on Pattern Analysis and Machine Intelligence*, 13(11), 1115–1138.

Tsai, Y., Ai, C., Wang, Z., and Pitts, E. (2013). "Mobile cross-slope measurement method using lidar technology." *Transportation Research Record: Journal of the Transportation Research Board*, 2367, 53–59.

Tsai, Y., Wu, J., Wang, Z., and Hu, Z. (2010). "Horizontal roadway curvature computation algorithm using vision technology." *Computer-Aided Civil and Infrastructure Engineering*, 25(2), 78–88.

List of Tables

TABLE 1. Confusion matrix for curve classification test

		Proposed Method			
		Simple Curve	Compound Curve	Reverse Curve	Spiral Curve
Ground Truth	Simple Curve (117)	90.6%	6.0%	0.0%	3.4%
	Compound Curve (103)	5.8%	86.4%	0.0%	7.8%
	Reverse Curve (78)	1.3%	0.0%	98.7%	0.0%
	Spiral Curve (49)	24.5%	12.2%	0.0%	63.3%

List of Figures

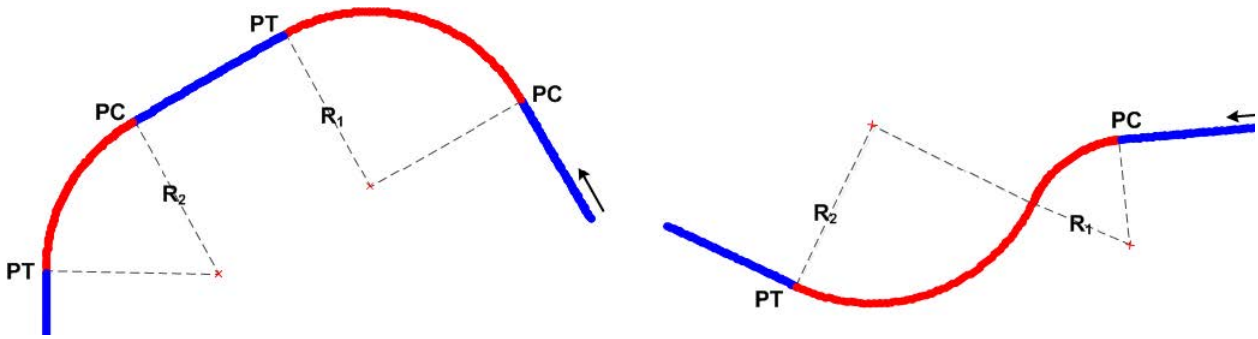

Fig. 1. Illustration of horizontal curves delineated by PC and PT

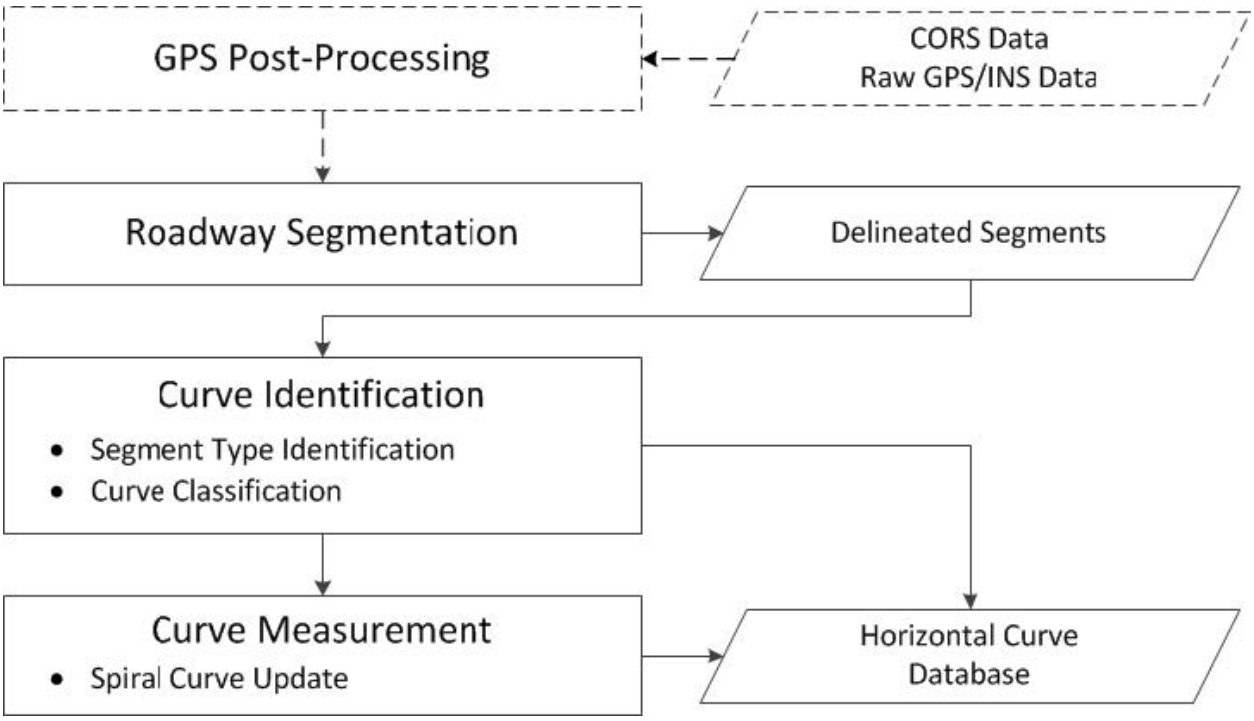

Fig. 2. Flowchart for the proposed automatic horizontal curve identification and measurement method

(a) **(b)**

Fig. 3. The data collection vehicle and the sample GPS trajectory data

PSEUDO CODE - ITERATIVE CIRCULAR FITTING

Input a GPS sequence (x, y)

Initialize the piece struct $L(\text{index}, \text{interval}, x_{center}, y_{center}, \text{Curvature}, \text{flag})$

for GPS point (x_i, y_i)

  for each interval j (incremental j)

    Compute circle center (a_{ij}, b_{ij}) and radius R_{ij} using Kasa circle fitting

    Compute error term $E_j = \frac{1}{j} \cdot \sum_{k=i}^{i+j} \left(\sqrt{\left((x_k - a_{ij})^2 + (y_k - b_{ij})^2 \right)} - R_{ij} \right)$

  end

  $m = \text{argmin}_j(E_j)$

  Add record of $L_n = L(i, m, a_{im}, b_{im}, R_{im}{}^{-1})$ to L

  $n = n + 1$

  $i = i + m + 1$

end

(a)

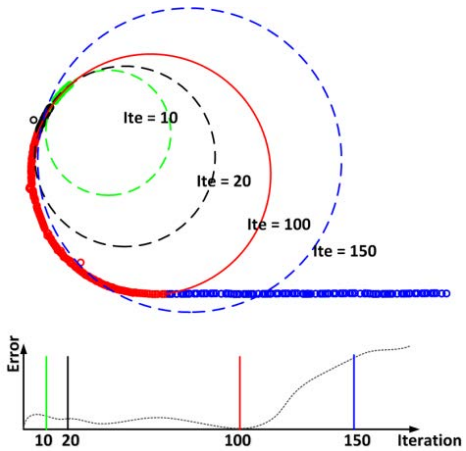

(b)

Fig. 4. Pseudo code and illustration for iterative circular fitting algorithm

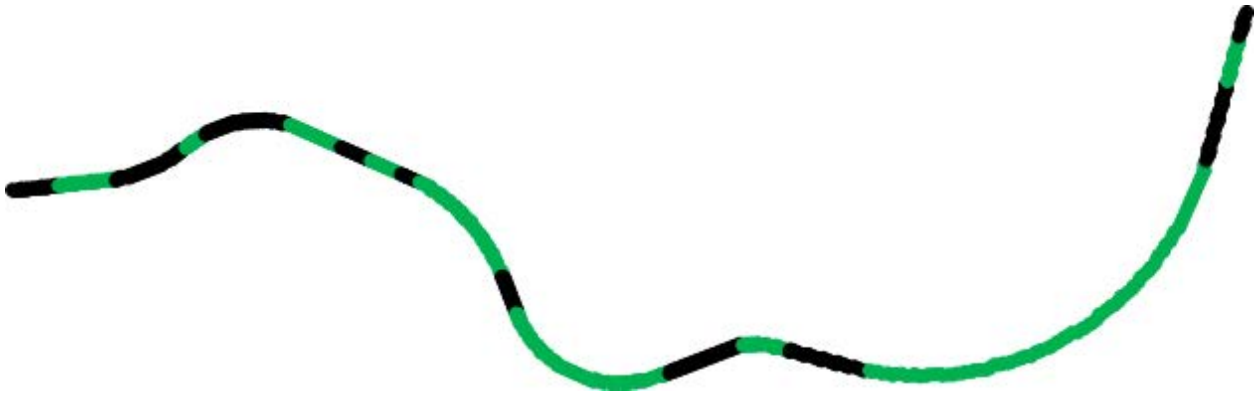

Fig. 5. Illustration of the resultant segments on a small road section

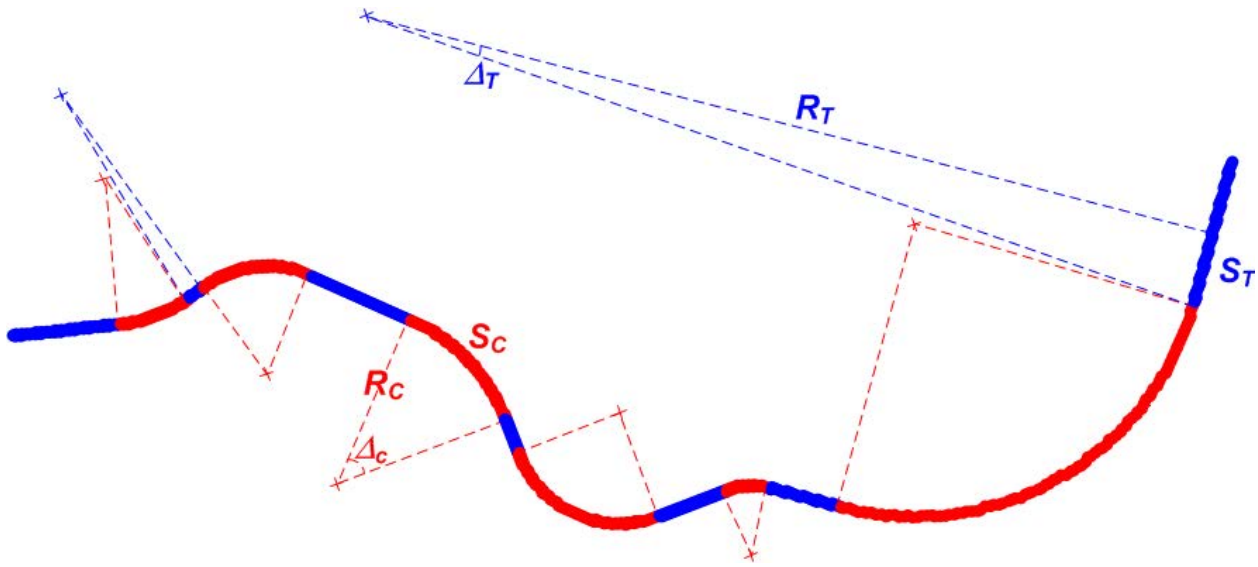

Fig. 6. Illustration of different center angles for curved and tangent segments

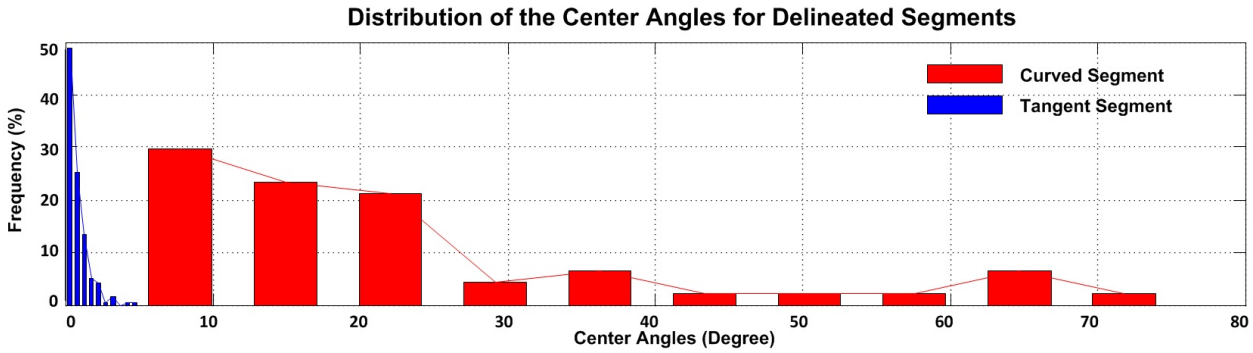

Fig. 7. Distribution of the center angles in the calibration dataset

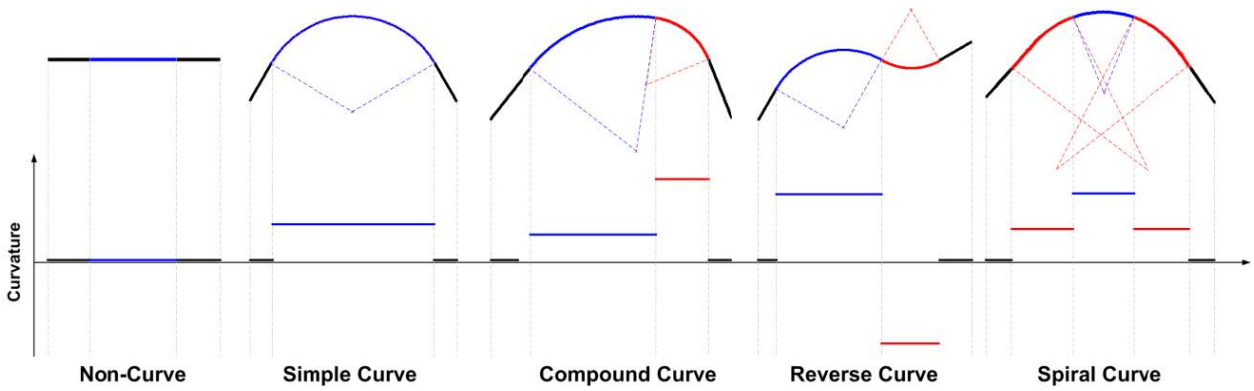

Fig. 8. Illustration of the segment adjacency patterns for different curve types

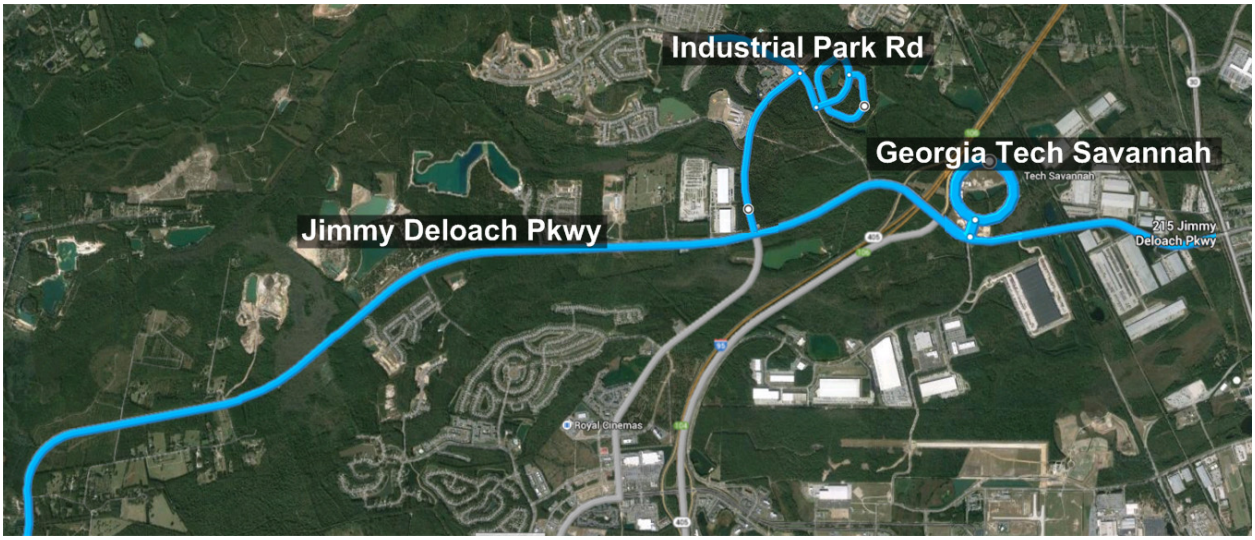

Fig. 9. Map of the selected roadway in the field test

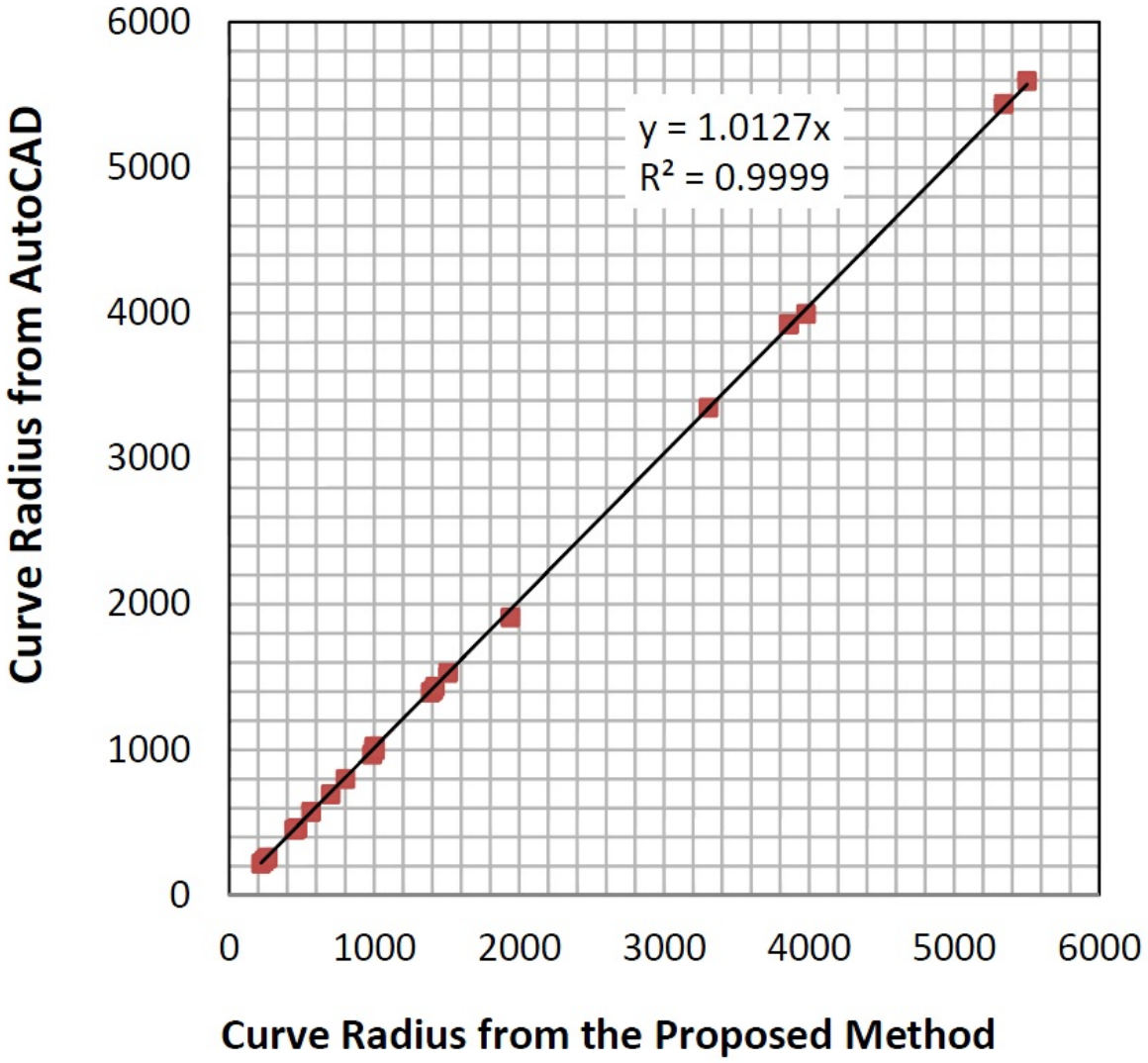

Fig. 10. Curve radius measurement results of the field test

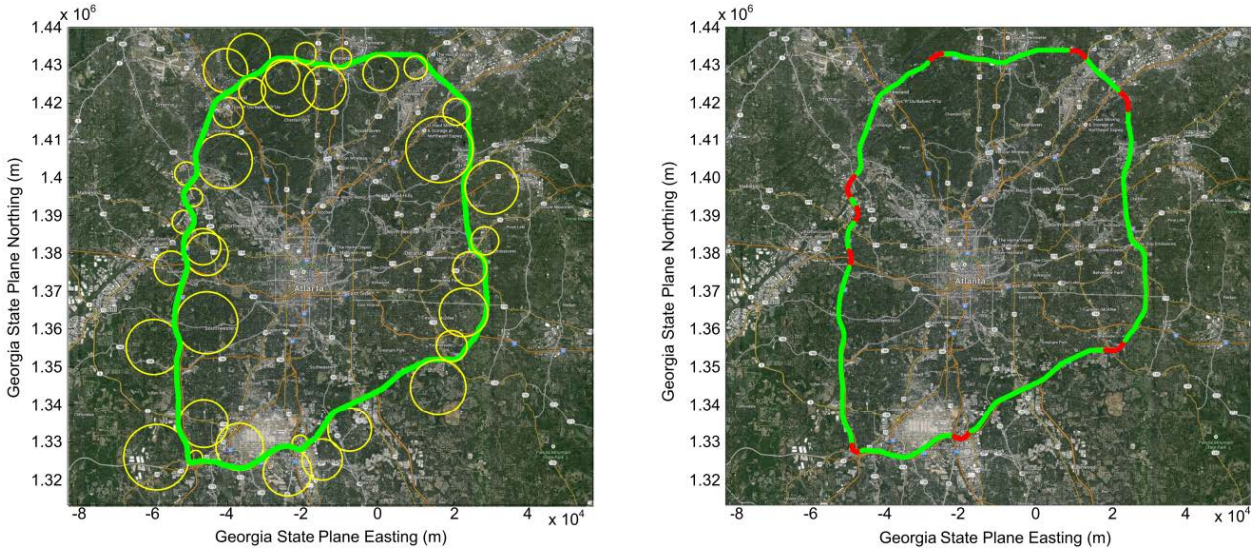

Fig. 11. Illustration of the identified locations of interest on I-285

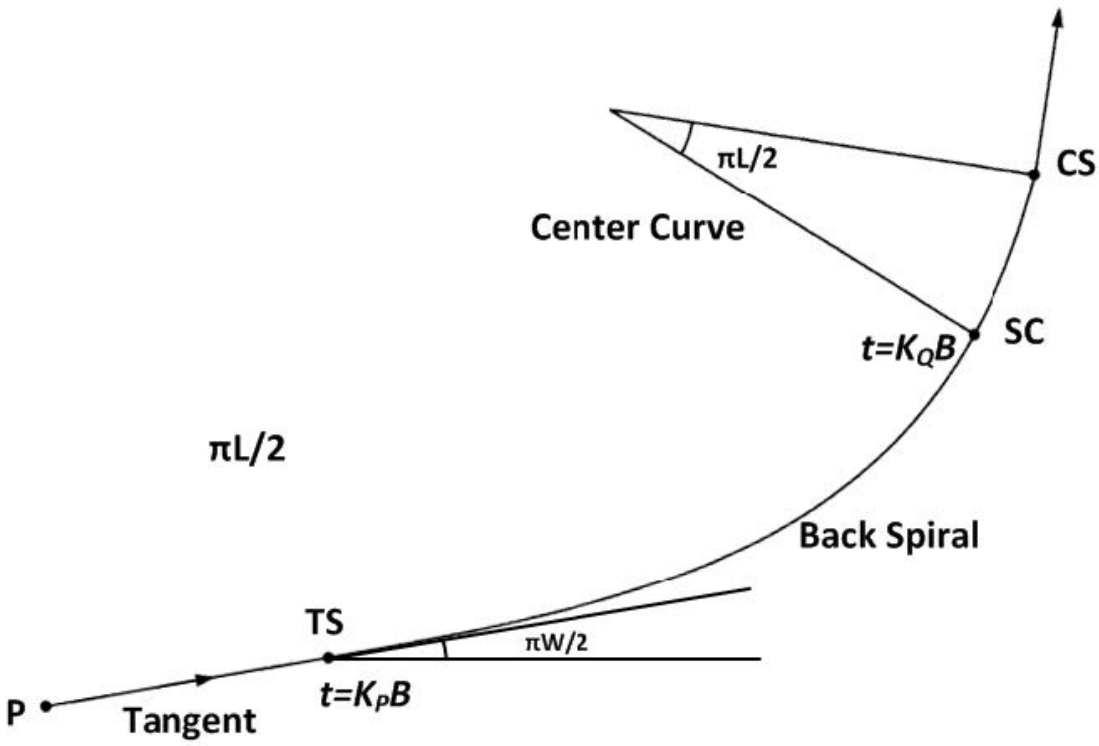

Fig. 12. Illustration of the Clothoid spline with a back spiral